Remote laser evaporative molecular absorption spectroscopy

Gary B. Hughes[a], Philip Lubin[b], Alexander Cohen[b], Jonathan Madajian[b], Neeraj Kulkarni[b], Qicheng Zhang[b], Janelle Griswold[b], and Travis Brashears[b]

gbhughes@calpoly.edu
lubin@deepspace.ucsb.edu

[a]Statistics Department, California Polytechnic State University, San Luis Obispo, CA 93407-0405
[b]Physics Department, University of California, Santa Barbara, CA 93106-9530

ABSTRACT

We describe a novel method for probing bulk molecular composition of solid targets from a distant vantage. A laser is used to melt and vaporize a spot on the target. With appropriate flux, the spot temperature rises rapidly, and evaporation of surface materials occurs. The melted spot creates a high-temperature blackbody source, and ejected material creates a plume of surface materials in front of the spot. Molecular and atomic absorption occurs as the blackbody radiation passes through the ejected plume. Bulk molecular and atomic composition of the surface material is investigated by using a spectrometer to view the heated spot through the ejected plume. The proposed method is distinct from current stand-off approaches to composition analysis, such as Laser-Induced Breakdown Spectroscopy (LIBS), which atomizes and ionizes target material and observes emission spectra to determine bulk atomic composition. Initial simulations of absorption profiles with laser heating show great promise for Remote Laser-Evaporative Molecular Absorption (R-LEMA) spectroscopy. The method is well-suited for exploration of cold solar system targets—asteroids, comets, planets, moons—such as from a spacecraft orbiting the target. Spatial composition maps could be created by scanning the surface. Applying the beam to a single spot continuously produces a borehole or trench, and shallow sub-surface composition profiling is possible. This paper describes system concepts for implementing the proposed method to probe the bulk molecular composition of an asteroid from an orbiting spacecraft, including laser array, photovoltaic power, heating and ablation, plume characteristics, absorption, spectrometry and data management.

Keywords: Directed Energy, Laser Phased Array, Asteroid Composition

1. INTRODUCTION

1.1. Asteroid Composition

Astronomical surveillance has identified more than 600 000 asteroids and comets, which are icy and rocky remnants of the formation of our solar system. Most of these objects remain in stable orbits around the Sun, within a 'main belt' between Mars and Jupiter; a schematic distribution is shown in Fig. 1. Main belt asteroids can sometimes be perturbed from their stable orbits, mainly through the process of Yarkovsky thermal drag[1], but occasionally through interaction with other asteroids or planets. Orbital perturbations can deflect asteroids toward the inner planets, including into paths that cross Earth's orbit. Asteroids that approach or cross Earth's orbit are deemed Near Earth Asteroids (NEAs). A slightly larger class, including asteroids and comets, is referred to as Near Earth Objects (NEOs). NEOs are best characterized as transient objects, *i.e.*, the average lifetime of NEOs is relatively short, perhaps only a few million years.[2] Objects that linger in the inner solar system are eventually removed or destroyed, either by direct collision with a planet or the Sun, or by ejection from the solar system via orbit alteration. The comet ISON appeared to disintegrate on 28 November 2013 when its orbit passed too close to the Sun.

From time to time, NEOs impact Earth, *e.g.*, on 15 Feb 2013, an asteroid that was 19.8±4.6 m wide barreled through the atmosphere and struck Earth near Chelyabinsk, Russia.[3] The airburst over Chelyabinsk released energy equivalent to 570±150 kt TNT.[3] For comparison, the nuclear bomb that was detonated in Hiroshima, Japan in 1945 yielded ~12.5 kt TNT.[4] The Chelyabinsk impact resulted in 1200 injuries, with property damage in the range US$33-50 million[3], caused by an asteroid that was not previously observed. In order to evaluate the threat posed to Earth and society, it is imperative that we continue efforts to discover more objects in the unknown population, and to characterize properties of potentially hazardous asteroids and comets. In addition to discovery and orbit determination, it is also crucial to understand the physical properties of bolides, particularly size and composition. Studying of asteroid composition also provides vital information to inquiries of solar system origins. Investigating asteroid composition will be crucial to efforts aimed at exploiting asteroids for their mineral resources.

Current knowledge of asteroid composition comes mainly from observations of reflected light over optical and near-infrared wavelengths.[5] Asteroids are classified within a taxonomy based on spectral characteristics of the reflected light, which derives primarily from properties of surface material. Occasionally, bulk composition can be studied directly when meteorites such as the Chelyabinsk impactor are recovered, providing additional insight about composition of objects in the spectral class to which the parent asteroid belonged. For many asteroids, light reflected from the surface can only divulge information about surface material, which is often a fine dust coating ('regolith') that may or may not be derived from, or representative of, the asteroid's bulk composition. Regolith may be altered material from the asteroid, or derived from collisions, or some combination thereof.

Direct sampling of asteroid and comet material has been limited to a few missions. The Hayabusa mission by the Japanese Aerospace Exploration Agency (JAXA) collected and returned samples from the surface of asteroid 25143 Itokawa.[6] The sample consisted of approximately 1 g of particles in the size range 10-100 μm, mainly from regolith. NASA's Deep Impact mission to comet 9P/Tempel sought to excavate sub-surface material by sending an impactor to the surface.[7] Emission spectra of the heated ejecta were obtained, and analyzed for composition.[8] NASA's Stardust mission navigated through the coma of comet 81P/Wild, and returned samples to Earth.[9] The European Space Agency's (ESA) Philae lander of the Rosetta mission analyzed surface samples of comet 67P/Churyumov–Gerasimenko, sending data recorded *in situ* on the comet back to Earth.[10] NASA's Osiris-Rex mission, with a launch window beginning on 08 September 2016, aims to rendezvous with asteroid 101955 Bennu, perform a 'touch-and-go' maneuver, and then return samples of surface material to Earth.[11,12]
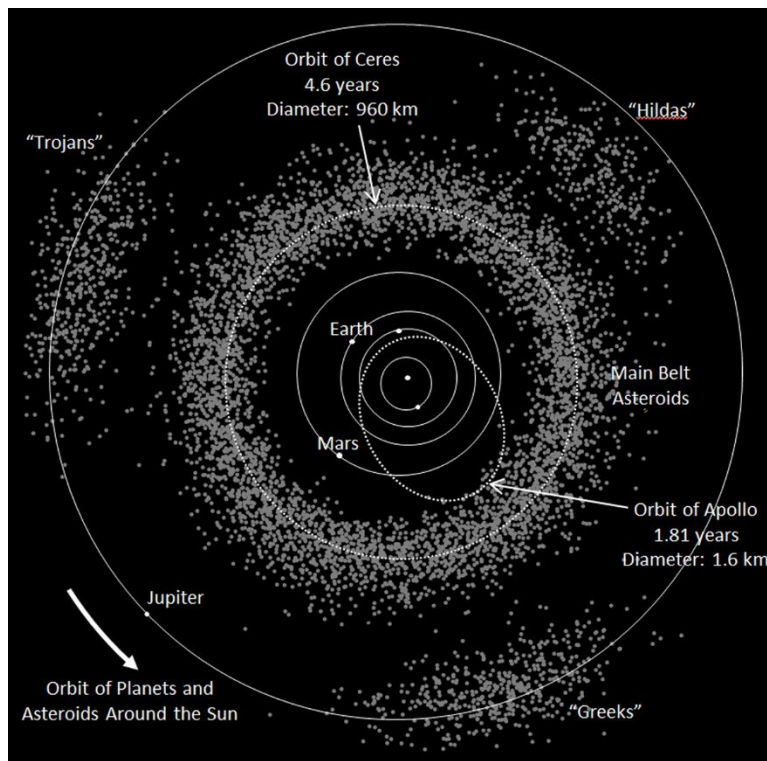

Figure 1. A schematic representation of main-belt asteroid orbits, looking downward onto the ecliptic plane. Main belt asteroids orbit the Sun between Mars and Jupiter. Ceres, with a mean diameter of 952 km, is the largest known asteroid, and is ensconced in a main-belt orbit. Main-belt objects can be deflected into the inner solar system, most often due to Yarkovsky thermal drag.[1]

1.2. A Concept for Remote Molecular Composition Analysis

Missions to directly assess asteroid composition are notable for their ingenuity and tenacity in the face of very difficult mission scenarios. Due to overall mission complexity, sample-return or landing/*in situ* measurement missions are likely to be limited in scope and number for the foreseeable future. We propose a novel method for probing the molecular composition of cold solar system targets (asteroids, comets, planets, moons) from a distant vantage, such as

from a spacecraft orbiting the object.[13,14] The spacecraft includes a solar-powered laser array. A directed energy beam from the laser is focused on the target. With target flux in the range of ~10 MW/m^2, the spot temperature rises rapidly, to ~2500 K for rocky targets, and melting and evaporation of surface materials on the target occurs. Material ejected from the heated spot creates a molecular plume of surface materials in front of the spot. Energy from the laser is insufficient to dissociate molecules or spawn significant ionization, so the plume retains the molecular composition of the target. The melted spot becomes a high-temperature blackbody source. As the blackbody radiation passes through the ejected plume, molecular and atomic absorption occur in the plume materials. Bulk molecular and atomic composition of the surface material is investigated by using a spectrometer to view the heated spot through the ejected material. A system concept is shown in Fig. 2.
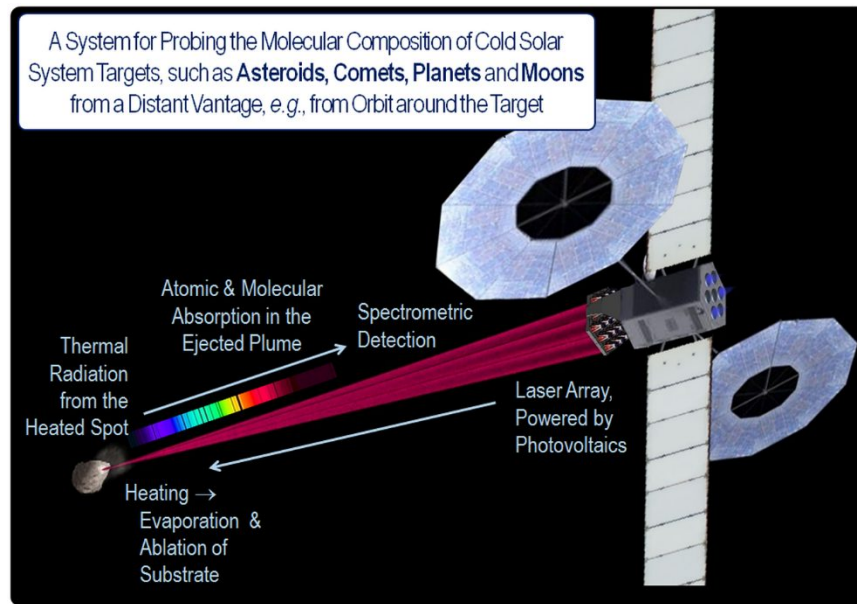

Figure 2. A system concept for probing bulk molecular and atomic composition of cold solar system targets, such as asteroids, comets, planets, moons, from a distant vantage, such as from a spacecraft orbiting the object.[13,14]

The R-LEMA tactic differs fundamentally from current 'stand-off' approaches for composition analysis. One currently used stand-off approach is Laser-Induced Breakdown Spectroscopy (LIBS).[15] This technology has been thrust into the public consciousness due to its deployment on of the Mars Curiosity rover.[16] LIBS uses a pulsed laser with optics that can focus on targets within ~10 m of the rover. The laser pulses deliver a flux exceeding 10 TW/m^2, which is sufficient to dissociate molecules and create an atomic plasma from materials in the solid target. Light emitted from the plasma is delivered to a series of three spectrometers covering the range 240-850 nm. Atomic composition is derived from the recorded spectra.[17] Standoff distance for LIBS on the Curiosity rover is limited by the strength of characteristic emission, and distances greater than ~10 m are problematic. Additionally, the LIBS detector performs atomic composition analysis by observing characteristic emission spectra from the plasma in visible and near-infrared (Vis/NIR) wavelengths.

Laser-Induced Thermal Emission (LITE) spectroscopy is also capable of probing molecular composition from moderate distances.[18] LITE uses a relatively low-power laser to heat materials in the target to a temperature that is perceptibly higher than the environment. An infrared imaging system focuses the target on an infrared spectrometer. Materials in the target emit blackbody radiation with diagnostic spectral features in infrared wavelengths that arise from rotational and vibrational movements of molecules. LITE spectroscopy is theoretically capable of operating at very large stand-off distances, limited mostly by laser power. LITE spectroscopy is typically limited to molecular composition analysis, due to low emitted signal in optical wavelengths, where characteristic emission occurs. A strategy similar to LITE was utilized by the Deep Impact mission. A large amount of material was ejected from the comet by the impact. The cloud of ejected debris was pushed by solar radiation pressure into the comet's coma. The ejected material is heated by solar radiation (rather than a laser) to ~235 K, and the heated material then emits blackbody energy peaking near 12 μm. 'Solar-illuminated emission spectra' in the range 5.2-38.0 μm were recorded from the Spitzer Space

Telescope in low-Earth orbit, at a distance of ~0.75 AU from the comet.[8] Molecular composition of materials in the coma was inferred from the mid- and long-wave infrared (MWIR and LWIR) spectra. These examples illustrate some of the various methods that can be used to exploit light-matter interaction for purposes of target composition analysis; a general depiction is shown in Fig. 3.
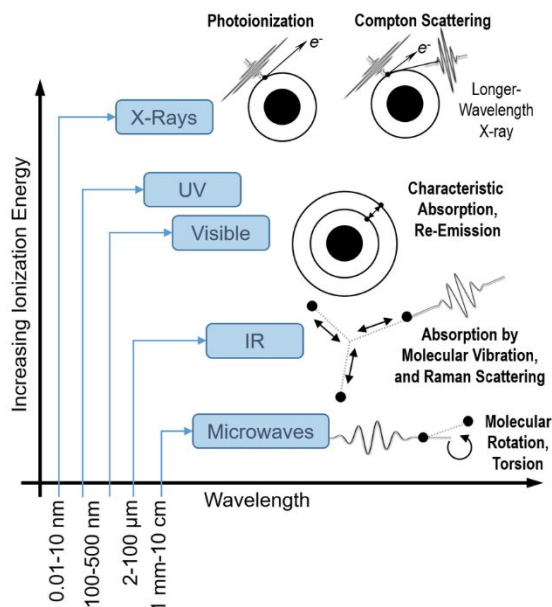

Figure 3. Various light-matter interactions can be exploited for purposes of target composition analysis.

R-LEMA differs from LIBS in several important ways. First, while LIBS detects emission spectra from the plasma, R-LEMA detects absorption lines in spectra from a 'backlight' blackbody source. The approach is similar in nature to molecular and atomic composition analysis of stellar and sub-stellar objects, which exploits absorption features in the back-light blackbody source.[19,20] Furthermore, R-LEMA proposes to deliver flux near ~10 MW/m^2, which is sufficient to melt and evaporate rocky materials, but insufficient to dissociate molecules. As such, the cloud of emitted material retains the molecular makeup of the target. It is therefore feasible to seek atomic and molecular composition of materials in the plume from Vis/NIR and MWIR/LWIR absorption spectra, respectively. Stand-off distance for R-LEMA is limited by the ability to point and focus a directed energy beam on the target with sufficient flux to evaporate surface materials, and by the opacity of the ejected material plume. Initial results indicate that, with currently available technology, stand-off molecular composition analysis is immediately feasible over distances greater than 100 km, and over much greater distances with modest advances in optical systems.[14] Results also indicate that R-LEMA is not feasible over distances less than ~30 m, due to limited optical path that is insufficient to produce discernible absorption. In this sense, R-LEMA and LIBS are complementary in regard to stand-off distance. Both systems could be installed on a lander to greatly extend the radius of exploration. The capability to probe surface materials at a greater distance could potentially overcome planetary protection concerns, and generally support exploration of areas that are inaccessible to the lander. R-LEMA is perhaps best suited to deployment on a spacecraft that would orbit the target.

This paper discusses system concepts for implementing R-LEMA in the context of probing the bulk molecular composition of an asteroid from an orbiting spacecraft. A hypothetical mission is envisioned, and spacecraft architecture for the mission scenario is described. Consider a spacecraft design with ~2 m diameter laser array, consuming ~100 kW electrical power. The hypothetical mission would orbit a target at 10-100 km, and deliver 10 MW/m^2 over a 0.01-0.10 m spot. In order to design an R-LEMA system for such a mission, theoretical assessments of system operation are described. Simulations have been developed for laser heating of a rocky target, with concomitant evaporation. Evaporation rates lead to determination of plume density and opacity. Absorption profiles for selected materials are estimated from plume properties. Initial simulations of absorption profiles with laser heating show great promise for molecular composition analysis from with currently available technology.

2. LASER ARRAY, POWERED BY PHOTOVOLTAICS

2.1. Spacecraft Architecture and Photovoltaic Power

For the hypothetical mission equipped with an R-LEMA spectrometer, the laser array is supplied ~100 kW electrical power from the photovoltaic (PV) panels. The basic design principle is to utilize a cylindrical bus with the lateral center of gravity close to the centerline.[21,22] PV panels will be stowed at the back of the bus until deployment, and the hexagonal laser array will be mounted on a gimbal at the front of the spacecraft (Fig. 4). Radiator panels will deploy up and down (perpendicular to the bus) and will rotate about their axis so as to remain perpendicular to the sun in order to maximize radiator efficiency. Two 15 m diameter MegaFlex PV arrays, manufactured by ATK Aerospace Systems in Goleta, CA, will be used to obtain the baselined 100 kW power solution. Extensive testing has been conducted on MegaFlex technology and the MegaFlex arrays have a high Technology Readiness Level (TRL).[23]
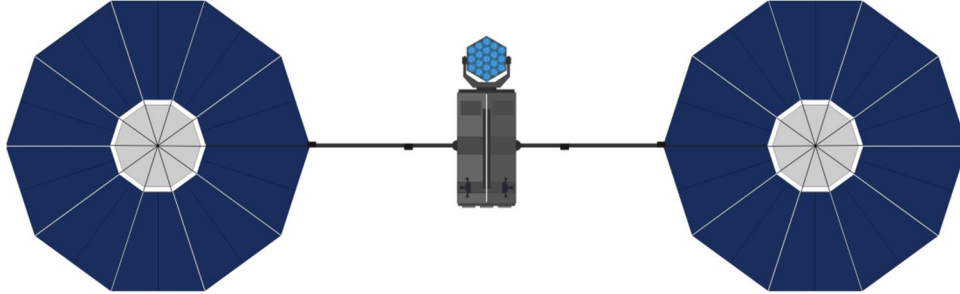

Figure 4. Conceptual design of the deployed spacecraft with two 15 m PV arrays that produce 50 kW each at the beginning of life for a total of 100 kW electrical, and the laser array pointed directly at the viewer. A 2 m diameter laser phased array is shown with 19 elements, each of which is 1-3 kW optical output.

2.2. Spacecraft Thermal Management

Thermal radiators are essential to spacecraft design so as to minimize incident radiation and maintain the spacecraft and its components at a functional temperature. The efficiency of the radiator can be determined by:

$$F = \frac{Q}{A} = \varepsilon \cdot \sigma \cdot T^4 \tag{1}$$

where ε is the emittance of the surface, σ is the Stephan-Boltzmann constant, T is the temperature, $Q^{\cdot}$ is the heat rejected, A is the area, and F is the flux.[24] The area of the radiator must be determined by thermal analysis, and is dependent on the desired operating temperature, heating from the environment, interactions with other surfaces of the spacecraft (e.g., solar arrays), and the highest estimate (worst case) satellite waste heat. The waste heat in this case is dependent on the efficiency of the laser amplifiers, ~35% to 50%. The worst-case estimate requires 65 kW to be rejected as waste heat for a 100 kW electrical input assuming virtually all the power goes to the laser (which is approximately correct during laser firing). The required area A is determined by:

$$Q_{rejected} = A \cdot F_{net} \tag{2}$$

where F_{net} is the net outward flux and $Q_{rejected}$ is the heat rejected. Given these parameters, the maximum required area of the radiator is ~341 m^2 for a 35% efficient laser amplifier. For a 50% efficient laser, a radiator area of ~262 m^2 is required. Both estimates assume that either a pumped liquid cooling loop or an advanced heatpipe would be used to transfer the heat from the laser to the radiator as is currently done in the other uses of these laser amplifiers.

A passive cooling z-folded radiator consisting of two deployable panels of 18 segments each will be used in order to provide a sufficient surface area over which to emit the waste heat generated by the system. The panels will rotate about their axes to maximize efficiency by remaining perpendicular to the sun and by radiating out of both sides. Each segment will be 2.2 m by 2.2 m, yielding a total area of 348 m^2. These values are approximate; a more detailed radiator design would be required as part of an overall mission design. By the time of any mission start, significant increases in laser efficiency will be expected, thus reducing the required radiator size.

2.3. Laser Architecture

The core idea of remote composition analysis relies on the ability to heat a distant target to the point of melting and evaporation. Advances in laser technology now allow contemplation of systems that are capable of delivering

sufficient flux to very distant targets. The performance of Ytterbium-doped fiber laser amplifiers has improved markedly in recent years. Continuous-wave, multi-kW-class devices are now routine and affordable, germinating many novel applications.[25,26] Coherently combined emitters are well-established.[27] Alternatively, multiple lasers could be arranged without phase alignment, and individual beams could be focused on adjacent spots on the target. Multi-beam 'tiled aperture' emitters are effective, but would be limited to closer targets than phased-array emitters with equivalent base power.

3. LASER HEATING AND THERMAL ANALYSIS

3.1. Beam Intensity Models

A model is presented for beam formation by a coherently-combined laser array, based on previous work.[28] Beam intensity models are used as input to thermal models of the target. The model is suitable for estimating far-field beam intensity, under some assumptions about the source of phase mis-alignment in a coherently-combined laser array. The interference pattern and resulting far-field intensity distribution of multiple emitters in a phased-array design can be determined by scalar diffraction theory. The complex far-field amplitude for a linear array of emitters with static (E_f) and time-varying (E_t) phase misalignments at each emitter is given by:

$$E(\theta, t) = \frac{e^{[i \cdot k \cdot a \cdot sin(\theta)]} - 1}{i \cdot k \cdot sin(\theta)} \cdot \sum_{p=0}^{N-1} e^{\{i \cdot [k \cdot p \cdot d \cdot sin(\theta) + E_f(p) + E_t(p,t)]\}} \tag{3}$$

Given the complex amplitude, the far-field beam intensity for the linear array is then:

$$I(\theta) = |E(\theta)|^2 \tag{4}$$

For a 1-D linear array, the far-field beam intensity for a square array with beam intensity $I_x(\theta)$ along one axis and $I_y(\psi)$ along a perpendicular axis is:

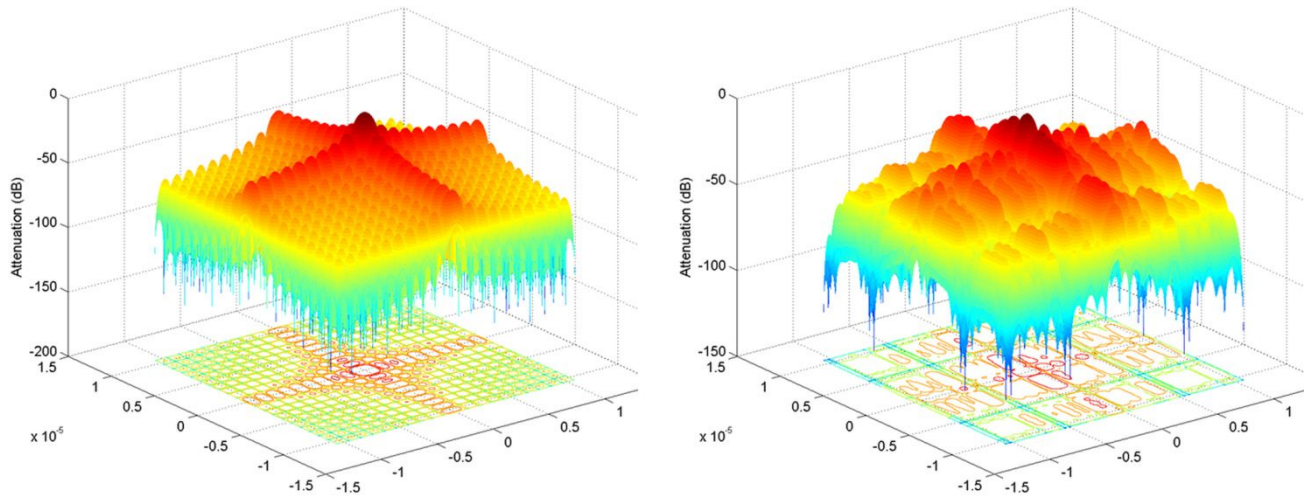$$I(\theta, \psi) = I_x(\theta) \cdot I_y(\psi) \tag{5}$$

Figure 4. Simulation results for a 5 by 5 close-packed array of emitters, showing far-field intensity. Emitters are modeled as a close-packed array with 20 cm pitch, total aperture is 1 m, and the nominal emitter frequency is 1.06 μm **Left**: No phase perturbations. **Right**: Static phase perturbations due to mechanical mis-alignments were randomly assigned to each emitter, with magnitudes drawn from a normal distribution with 1σ = 2π/8.

The simulation results shown in Fig. 4 represent a laser phased array far field intensity, based on Eq. (3)-(5). A simulation was run without phase perturbations. Simulations were also run that include fixed phase mis-alignments (E_f) at each emitter with a 1σ error of λ/8. Comparison of the two simulations shows significant beam degradation, with power moving from the main peak to side lobes. Also evident is a pointing shift, *i.e.*, the main lobe axis is no longer aligned with the array axis, with a pointing error on the order of 1 μrad.

3.2. Thermal Analysis

To investigate the feasibility of R-LEMA, models of the thermal progression of bolides being bombarded with laser energy have been developed. Simulations include coherently combined laser arrays and tiled-aperture configurations. Model results are present a theoretical foundation that supports the proposed method.[13,14,21]
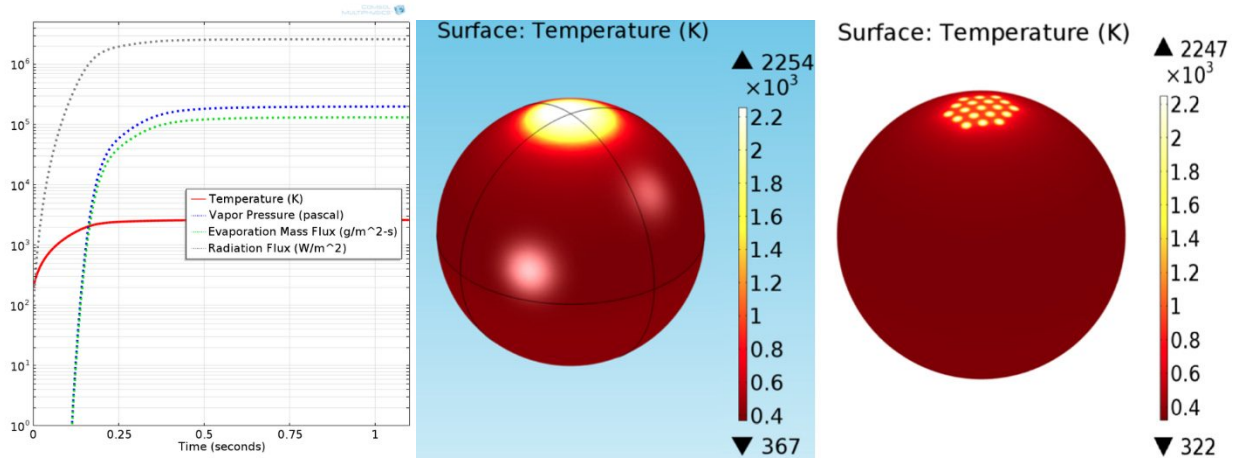

Figure 5. Results from a multi-physics model of a spherical bolide of micro-crystalline Silica (SiO_2).[21] Model features include radiation, conduction and mass ejection. **Left:** Conceptual illustration of a directed energy beam impinging on an asteroid; surface material is ejected from the heated spot, creating a plume. **Center:** Simulation results showing steady-state condition, under illumination with a single beam produced by an array of coherently combined lasers. **Right:** The same bolide, under illumination with tiled aperture emitter.

4. EVAPORATION AND ABLATION OF THE SUBSTRATE

4.1. Surface Material Ejection

The energy required to vaporize materials on the surface of an asteroid is determined by the heat of fusion and required increase in temperature to bring the surface material to the melting point from (assumed) initial low temperature starting point. Fig. 6 shows the relationship between vapor pressure in Pascals (N/m^2) versus Temperature, and versus target flux, for several compounds that are thought to be common in asteroids.[3,10] The typical energy per m^3 is on the order of 10^{10} J to vaporize most materials. At temperatures exceeding ~2250 K, which occurs at fluxes greater than ~10 MW/m^2, the vapor pressures of all compounds are very high. That is, none of these materials remain solid, and mass ejection rates will be high. Even vapor pressures in the range of 10^3 Pa (0.01 atmospheres) correspond to large mass ejection rates. The curves in Fig. 6 are applicable to the worst case of complete chemical binding (*i.e.*, solid). In contrast to the small iron-rich meteorites that are sometimes found on the ground, a more typical asteroid likely has much lower thermal conductivity, for example in cases where the asteroid is an agglomeration of smaller fragments (a "rubble pile" asteroid). In many cases asteroids, will have significant amounts of low temperature volatile materials that lower the power requirements for evaporation of surface material. Asteroids are also molecular rather than atomic in species in general, but the conclusion are the same, namely at temperatures in the range of 2000 to 3000 K or target fluxes in the range 106 to 108 W/m^2, all known materials will undergo vigorous evaporation. What is critical is to increase the spot flux to the point where evaporation becomes large. It is not sufficient to simply apply a large amount of total power, there has to be a large flux to initiate evaporation.

4.2. Material Properties

Mass ejection from a solid that is heated is analogous to evaporation of a liquid, except in many circumstances the solid material is effectively sublimating. The effective vapor pressure of the material being ejected is essentially in equilibrium though in the case of an asteroid, surface evaporation or sublimation is a pure equilibrium process as the material streams into the hard vacuum of space. This process is similar but critically different than a constant temperature case where the mass ejection rate is temperature limited by the constant bath temperature. In the case of a laser beam striking the surface of an asteroid in space, the laser adds energy to the material and this is counteracted by

the outgoing energy channels of surface reflection, scattering and absorption in the ejecta, mass ejection, radiation and thermal conductivity. This is somewhat different than the constant temperature case where the mass ejection stops increasing when the vapor pressure is limited by the temperature. The laser heats the material to the point where the increase in temperature is balanced by the energy loss due to all other processes. In particular the surface effects (Knudsen layer) are different as the temperature will increase to the point where energy equilibrium is achieved. This is different than the constant temperature case where thermal equilibrium at the constant temperature is achieved. Fig. 3 illustrates several cases for typical compounds present in asteroids both vs. temperature and flux. The analysis for each compound is calculated as below.
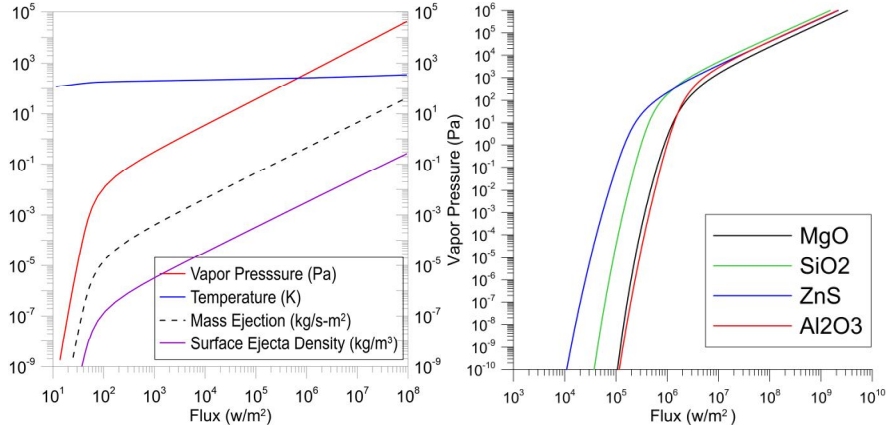

Figure 6. **Left**: Vapor pressure, temperature, mass flux and vapor surface density vs. Flux. Right: Vapor pressure vs. target flux for four common high temperature asteroid compounds. For water at flux exceeding ~1 kW/m², the vapor pressure and hence mass ejection rises rapidly; for the high temperature compounds, this occurs at fluxes exceeding 10 MW/m².

4.3. Mass Ejection

To calculate the mass ejection, use Langmuir's equation for evaporation. The particle ejection rate, or evaporative flux, I_e (molecules m^{-2} s^{-1}) is given by:

$$I_e = \frac{\alpha_e (P_v - P_h)}{\sqrt{2\pi m k T}} = \frac{\alpha_e N_A (P_v - P_h)}{\sqrt{2\pi M R T}} \tag{6}$$

The mass flux Γ_ε (kg m^{-2} s^{-1}) is found from the Langmuir equation Eq. (1):

$$\Gamma_e = I_e m = \frac{m \alpha_e (P_v - P_h)}{\sqrt{2\pi m k T}} = \frac{M \alpha_e (P_v - P_h)}{\sqrt{2\pi M R T}} = \alpha_e P_v \sqrt{\frac{M}{2\pi R T}} = \frac{\alpha_e P_v}{\upsilon_{AV} \pi / 2} = \frac{\alpha_e P_v}{\upsilon_e} \tag{7}$$

The mass flux (in kg m^{-2} s^{-1}) is

$$\Gamma_e = 0.138 \alpha_e \sqrt{\frac{M}{T}} (P_v - P_h) \tag{8}$$

4.4. Vapor Pressure

The vapor pressure of each element or compound can be computed from its associated Antoine coefficients (A, B, C). Based on the computed vapor pressures, the mass ejection flux can be determined for the full 3D and 4D cases numerically.[14] Note that in most cases, the Antoine coefficients are computed for Celsius temperature, and pressures are reported in mm Hg:

$$\left(P_v \right)_{Hg} = 10^{\left[\frac{A-B}{(T)_C - C} \right]} \tag{9}$$

5. PHYSICS OF MOLECULAR LINE ABSORPTION

5.1. Absorption Lines

As a laser beam strikes the surface of a target, two important things happen. The surface is heated, creating a blackbody source; and, material is ejected from the surface into the surrounding space. A mass ejecta cloud forms in the space between the laser source and the target, providing an opportunity to observe the molecular absorption lines as the blackbody energy passes through the ejecta cloud. Typically, during evaporation or sublimation, the material coming off the target is not ionized and the spot temperatures are low enough that infrared vibrational and rotational lines are observed.[30,31] The computed and measured absorption lines can be used to determine the observed spectra, as follows. At the surface of the spot:

$$B(\lambda) \ (w/m^2 - m) = c\rho(\lambda)/4 \tag{10}$$

$$F(\lambda) \ (w/m^2 - st - m) = B(\lambda)/\pi = c\rho(\lambda)/4\pi \tag{11}$$

$$N(\lambda) \ (\gamma/m^2 - s - st - m) = F(\lambda)/h\nu \tag{12}$$

where $F(\lambda)/h\nu$ is the photon flux at the surface of the spot. The spectral absorption lines due to molecular absorption can be calculated. The ejecta density, in molecules per cubic meter, is given by:

$$n'(z,R) = \frac{4\Sigma}{v}[(1-(R^2/z^2+1)^{-1/2}] \tag{13}$$

Where Σ is the ejecta flux, in molecules m^{-2} s^{-1} from the spot. The observed photon rate received per unit bandwidth by the telescope $G(\lambda)$ in γ s^{-1} m^{-1} is calculated form the observed photon flux at the telescope $H(\lambda)$ and the spot area of the asteroid:

$$G(\lambda) = H(\lambda) \cdot A_T \tag{14}$$

Let $\sigma(\lambda)$ be absorption cross section (in m^2 $atom^{-1}$). Then, $\tau(\lambda)$ is the integrated absorption line coefficient:

$$\sigma(\lambda)\int_0^L n'(z,R)dz \tag{15}$$

and the observed photon rate is:

$$G(\lambda) = \frac{A_{spot}A_T}{4\pi L^2} N(\lambda)\exp[-\int_0^L n'(z,R')\sigma(\lambda)dz] = \frac{A_{spot}A_T}{4\pi L^2} N(\lambda)e^{-\tau(\lambda)} \tag{16}$$

The absorption coefficient as a function of wavelength $\tau(\lambda)$ is given by:

$$\tau(\lambda) = n\sigma(\lambda)X = \frac{4\Sigma\sigma(\lambda)}{\upsilon}R \tag{17}$$

where n is an effective density and X is an effective length, the following relationships hold:

$$n = \frac{4\Sigma}{\upsilon} \text{ and } X = R \tag{18}$$

These relationships are reasonable, since it follows that $\Sigma = n\,v/4$ which makes sense. The effective length $X = R$, which is just the spot radius, hence:

$$\tau(\lambda) = n\sigma(\lambda)R \tag{19}$$

5.2. Spectrometry

It is now possible to compute the observed spectrum (rate received) $G(\lambda)$ (γ s^{-1} m^{-1}) and (flux received) $H(\lambda)$ (γ m^{-2} s^{-1} m^{-1}) as measured by a spectrometer as follows:

$$H(\lambda) = \frac{G(\lambda)}{A_T} \qquad (20)$$

$$\Omega_T = \frac{A_T}{4\pi L^2} \qquad (21)$$

Assuming the heated spot is a blackbody with temperature T for simplicity, with spectral radiance of $N_\lambda = N(\lambda)$ emitted at the spot, then the spectral density at the spot is:

$$\rho_\lambda = \frac{8\pi hc}{\lambda^5 \cdot (e^{hc/\lambda kT} - 1)} \qquad (22)$$

It is now possible to calculate the observed spectra $G(\lambda)$:

$$G_\lambda = N(\lambda) A \Omega_T e^{-\tau(\lambda)} \qquad (23)$$

where the optical depth and surface spot density are:

$$\tau(\lambda) = 4\Sigma \sigma(\lambda) R / \upsilon = n_0 \sigma(\lambda) R \qquad (24)$$

$$n_0 = 4\Sigma / \upsilon \qquad (25)$$

The calculated cross sections for two molecular species, water and silica (SiO), are shown as examples in Fig. 7.
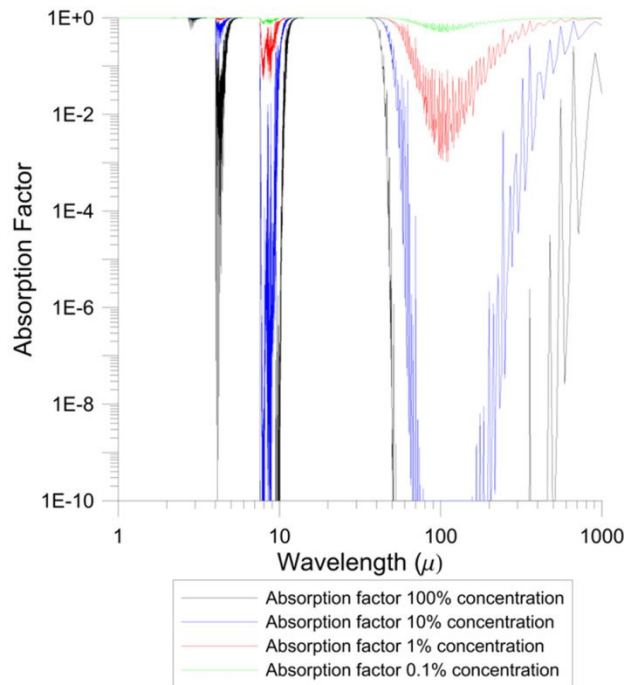

Figure 7. Since an asteroid will not be completely made of SiO, the absorption spectrum is computed for fractional compositions of 0.1 to 100% SiO to give an indication of the sensitivity to fractional composition. The "absorption factor" is the fractional composition of SiO.

6.   CONCLUSIONS

Laser-induced mass ejection can be used to remotely interrogate the molecular and atomic composition of a distant target. The feasibility of such a measurement depends on the details of the molecular cross section of the material in question and the laser power and distance to the target. Examples described in this paper indicate the

possible sensitivity of this method for long range detection. The determination of the composition of asteroids and other targets allows for future resource extraction by pre determining the materials in the target before visiting it. This is one example of the system. More materials are being investigated for remote analysis as are various system designs to determine practical methods of carrying out such surveys. Resource extraction in the solar system will become increasingly important and standoff molecular composition analysis is one method to aid in this endeavor.

ACKNOWLEDGEMENTS

REFERENCES

[1]   Morbidelli, A. "Asteroid Population Models, Dynamics of Populations of Planetary Systems," *Proceedings IAU Colloquium No. 197*, Z. Kneˇzeviˊc and A. Milani, eds. (2005).

[2]   Gladman, B.J., Migliorini, F., Morbidelli, A., Zappala, V., Michel, P., Cellino, A., Froeschle, C., Levison, H.F., Bailey, M. and Duncan, M. "Dynamical lifetimes of objects injected into asteroid belt resonances," *Science*, 277(5323), pp.197-201 (1997).

[3]   Popova, O.P., Jenniskens, P., Emel'yanenko, V., *et al*. Chelyabinsk Airburst, Damage Assessment, Meteorite Recovery, and Characterization, *Science*, 342(6162), 1069-1073 (2013).

[4]   Glasstone, S., and Dolan, P. "The Effects of Nuclear Weapons, Third Edition," Washington: Department of Defense, ch. 2 (1977).

[5]   DeMeo, F.E., Binzel, R.P., Slivan, S.M. and Bus, S.J. "An extension of the Bus asteroid taxonomy into the near-infrared," *Icarus*, 202(1), pp.160-180 (2009).

[6]   Yoshikawa, M., Fujiwara, A. and Kawaguchi, J.I. "Hayabusa and its adventure around the tiny asteroid Itokawa," *Proceedings of the International Astronomical Union*, 2(14), pp.323-324 (2006).

[7]   A'Hearn, M.F., Belton, M.J.S., Delamere, W.A., Kissel, J., Klaasen, K.P., McFadden, L.A., Meech, K.J., Melosh, H.J., Schultz, P.H., Sunshine, J.M. and Thomas, P.C. "Deep impact: excavating comet Tempel 1," *Science*, *310*(5746), pp.258-264 (2005).

[8]   Lisse, C.M., VanCleve, J., Adams, A.C., A'hearn, M.F., Fernández, Y.R., Farnham, T.L., Armus, L., Grillmair, C.J., Ingalls, J., Belton, M.J.S. and Groussin, O. "Spitzer spectral observations of the Deep Impact ejecta," *Science*, 313(5787), pp.635-640. (2006).

[9]   Brownlee, D., Tsou, P., Aléon, J., Alexander, C.M.D., Araki, T., Bajt, S., Baratta, G.A., Bastien, R., Bland, P., Bleuet, P. and Borg, J. "Comet 81P/Wild 2 under a microscope," *Science*, 314(5806), pp.1711-1716 (2006).

[10]   Glassmeier, K.H., Boehnhardt, H., Koschny, D., Kührt, E. and Richter, I. "The Rosetta mission: flying towards the origin of the solar system," *Space Science Reviews*, 128(1-4), pp.1-21 (2007).

[11]   Lauretta, D.S. and Team, O.R. "An overview of the OSIRIS-REx asteroid sample return mission," *Lunar and Planetary Science Conference*, Vol. 43, p. 2491 (2012).

[12]   Berry, K., Suttery, B., Mayz, A., Williams, K., Barbee, B.W., Beckman, M., and Williams, B. "OSIRIS-REx Touch-And-Go (TAG) mission design and analysis," in: *36th Annual AAS Guidance and Control Conference, AAS* 13-095 (2013).

[13]   Lubin, P., Hughes, G.B., Bible, J., Bublitz, J., Arriola, J., Motta, C., Suen, J., Johansson, I., Riley, J., Sarvian, N., Clayton-Warwick, D., Wu, J., Milich, A., Oleson, M., Pryor, M., Krogen, P., Kangas, M., and O'Neill, H. "Toward Directed Energy Planetary Defense," *Optical Engineering*, Vol. 53, No. 2, pp 025103-1 (2014).

[14] Hughes, G.B., Lubin, P., Meinhold, P., O'Neill, H., Brashears, T., Zhang, Q., Griswold, J., Riley, J., and Motta, C. "Stand-off molecular composition analysis," *Nanophotonics and Macrophotonics for Space Environments IX*, edited by Edward W. Taylor, David A. Cardimona, Proc. of SPIE Vol. 9616, pp. 961603 (2015).

[15] Miziolek, A.W., Palleschi, V., and Schechter, I. (Eds.). *Laser Induced Breakdown Spectroscopy (LIBS): Fundamentals and Applications*. New York: Cambridge University Press, ISBN 978-0-521-85274-6 (2006).

[16] Sallé, B., Lacour, J.L., Vors, E., Fichet, P., Maurice, S., Cremers, D.A. and Wiens, R.C. "Laser-induced breakdown spectroscopy for Mars surface analysis: capabilities at stand-off distances and detection of chlorine and sulfur elements," *Spectrochimica Acta Part B: Atomic Spectroscopy*, 59(9), pp.1413-1422 (2004).

[17] Sallé, B., Cremers, D.A., Maurice, S. and Wiens, R.C. "Laser-induced breakdown spectroscopy for space exploration applications: Influence of the ambient pressure on the calibration curves prepared from soil and clay samples," *Spectrochimica Acta Part B: Atomic Spectroscopy*, 60(4), pp.479-490 (2005).

[18] Lin, L.T., Archibald, D.D., and Honigs, D.E. "Preliminary Studies of Laser-Induced Thermal Emission Spectroscopy of Condensed Phases," *Appl. Spectrosc.* 42(3), 477-483 (1988).

[19] Bernath, P.F. "Molecular Astronomy of Cool Stars and Sub-Stellar Objects," *International Reviews in Physical Chemistry*, 28:4, pp. 681-709 (2009).

[20] Bernath, P.F. *Spectra of Atoms and Molecules, Second Edition*. New York: Oxford University Press, 439 p., ISBN 9780195177596 (2005).

[21] Kosmo, K., Pryor, M., Lubin, P., Hughes, G.B., O'Neill, H., Meinhold, P., Suen, J., C., Riley, J., Griswold, J., Cook, B.V., Johansson, I.E., Zhang, Q., Walsh, K., Melis, C., Kangas, M., Bible, J., Motta, Brashears, T., Mathew, S. and Bollag, J. "DE-STARLITE-a practical planetary defense mission," *Nanophotonics and Macrophotonics for Space Environments VIII*, edited by Edward W. Taylor, David A. Cardimona, Proc. of SPIE Vol. 9226 (2014).

[22] Lubin, P., Hughes, G.B., Eskenazi, M., Kosmo, K., Johansson, I., Griswold, J., Pryor, M., O'Neill, H., Meinhold, P., Suen, J., Riley, J., Zhang, Q., Walsh, K.J., Melis, C., Kangas, M., Motta, C. and Brashears, T. "Directed Energy Missions for Planetary Defense," *In Press*: Advances in Space Research, doi: http://dx.doi.org/10.1016/j.asr.2016.05.021 (2016).

[23] Murphy, D.M., Eskenazi, M.I., McEachen, M.E. and Spink, J.W. "UltraFlex and MegaFlex–Advancements in Highly Scalable Solar Power," In: *3rd AIAA Spacecraft Structures Conference*, p. 1947 (2016).

[24] Aaron, K. *Spacecraft Thermal Control Handbook, Volume 1: Fundamental Technologies*, The Aerospace Press, El Segundo, CA, ch. 6 (2002).

[25] Zervas, M.N. and Codemard, C.A. "High power fiber lasers: a review." *IEEE Journal of Selected Topics in Quantum Electronics*, vol. 20, no. 5, pp. 219-241 (2014).

[26] Wagner, T.J. "Fiber laser beam combining and power scaling progress: Air Force Research Laboratory Laser Division." *SPIE LASE*, pp. 823718-823718. Proc. of SPIE vol. 8237 (Feb. 2012).

[27] Vorontsov, M.A., Weyrauch, T., Beresnev, L.A., Carhart, G.W., Liu, L. and Aschenback, K. "Adaptive Array of Phase-Locked Fiber Collimators: Analysis and Experimental Demonstration," *IEEE Journal of Selected Topics in Quantum Electronics*, vol. 15, 269 (2009).

[28] Hughes, G.B., Lubin, P., Griswold, J., Bozinni, D., O'Neill, H., Meinhold, P., Suen, J., Bible, J., Riley, J., Johansson, I., Pryor, M. and Kangas, M. "Optical modeling for a laser phased-array directed energy system," *Nanophotonics and Macrophotonics for Space Environments VIII*, edited by Edward W. Taylor, David A. Cardimona, Proc. of SPIE Vol. 9226 (2014).

[29] Barton, E. J., Yurchenko, S. N., and Tennyson, J. "ExoMol line lists–II. The Ro-Vibrational Spectrum of SiO," *Monthly Notices of the Royal Astronomical Society*, vol. 434(2), pp. 1469-1475 (2013)

[30] Tennyson, J. and Yurchenko, S.N. "ExoMol: molecular line lists for exoplanet and other atmospheres," *Monthly Notices of the Royal Astronomical Society* vol. 425, pp. 21-33 (2012).

[31] Hill, C., Yurchenko, S.N. and Tennyson, J. "Temperature-dependent molecular absorption cross sections for exoplanets and other atmospheres," *Icarus* vol. 226, pp. 1673-1677 (2013).